JOURNAL OF COMPUTATIONAL PHYSICS 7, 102–119 (1971)

On the Numerical Solution of a Heat Equation Associated with a Thermal Print Head. II

JOHN LL. MORRIS

Department of Mathematics, University of Dundee, Dundee, Scotland

Received May 19, 1970

One of the variety of Hopscotch methods is considered for the numerical solution of a heat equation with variable coefficients defining the heat flow in a thermal print head. The associated heat source term is unusual in that it contains a branch point in the interior of the print-head as well as discontinuities of the space and time variables. Several numerical examples are discussed and the resulting behaviour of the difference scheme reported.

1. INTRODUCTION

In Ref. [10] we considered the numerical solution of a heat equation which arose when considering the mathematical model of a thermal print head. This heat equation was unusual in that the three-space-dimensional partial differential equation had, as one of the boundary conditions, a heat equation in two space variables. This partial differential equation contained a source term which was a discontinuous function of the time and space variables. The methods used in Ref. [10] were of the Alternating Direction and Locally One-Dimension types. It was concluded there that these schemes were reliable and accurate but, for physical problems under consideration, time consuming.

In the present paper, we will again consider a thermal print head which is structured similarly to the model described in Ref. [10]. There are, however, some fundamental differences. First, the three-dimensional print head we consider now has no *physical* heating element embedded within the surface material. In this model, heat is generated by an incident normal beam of electrons. This electron beam is active as a pulse with pulse width t_0 so that after t_0 sec the beam is switched off until such time as heat generation in the print head is required again.

A second difference between the model of print head we consider here and that described in Ref. [10] is that there, the surface film was considered to be so thin and thermal conductivity to be sufficiently large to allow us to neglect the tempera-

ture gradient normal to the surface. This then gave us the unusual set of equations alluded to earlier. Here the thermal print head has again two adjacent materials; one a good heat conductor and the other a poorer conductor. However, we do not assume the temperature gradient in the good conductor normal to the surface to be zero. Consequently, we obtain a single heat equation in three space dimensions to solve, with familiar-looking boundary conditions of the Dirichlet, Neumann, and Third boundary type.

The particularly interesting feature of this model, however, is the form of the heat source term which arises out of the incident electron beam. As in Ref. [10], the heat source term is a discontinuous function of the space variables x and y and the time t. The source term has a positive value for a finite depth in the print head but at one point has a "branch point," i.e., at a certain value of z the source term becomes infinite and for larger values of z becomes zero. It is this point which gives rise to possible difficulties.

The subject of this paper is, therefore, to consider some novel methods for the solution of partial differential equations of parabolic type (see Friedman, Ref. [3]) which have arisen out of work originally performed by Gordon [4] and, more recently, Gourlay [5, 6]. These schemes are a departure from the now more conventional methods of alternating direction, yet are ones we think have a great deal to offer to the practical numerical analyst.

The mathematical model is formulated and described in the next section. The difference schemes are discussed in Section 2. Several numerical experiments were carried out and are described in Section 4. The paper is concluded in Section 5.

2. The Physical Problem and its Associated Mathematical Formulation

A thermal print head, shown in Figs. 1 and 2, is a matrix of elements comprising a glass substrate upon which a thin film of a good heat-conducting material is deposited. The thin film has a small coefficient of specific heat and consequently reacts quickly to any change which occurs in a heat source. In contrast, the glass substrate has a smaller coefficient of conductivity and a higher coefficient of specific heat so that the substrate acts as a heat sink.

When the electron beam is projected normally onto the element, heat is produced. The surface element heats up quickly and, on passing a heat-sensitive paper across the surface, a chemical reaction will take place, if the temperature is high enough. By suitable combinations of the elements being heated, characters can be produced on the heat-sensitive paper. This is therefore a means of printing on paper without involving mechanical moving parts. The speed at which printing can occur depends upon the thermal properties of the print head. If the materials used are such that persistent switchings on and off of the heat source causes an

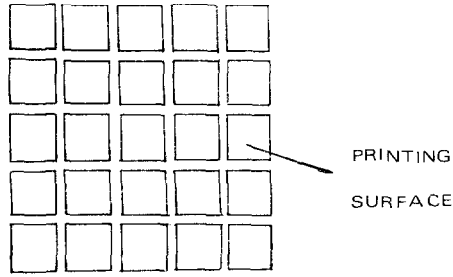

FIG. 1. A 5 × 5 matrix thermal print head (top view).

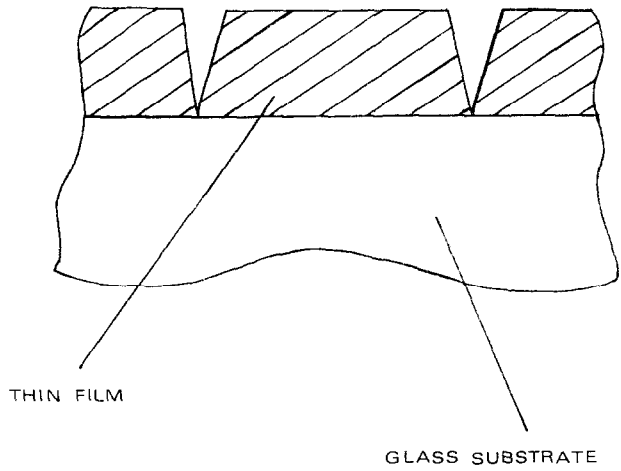

FIG. 2. A single element of the matrix (side view).

overall rise in temperature in the elements, a smudging effect of the characters will be produced which will ultimately merge into an indistinguishable mess. However, it is required to print separate characters as quickly as possible. Consequently, to investigate possible models with differing thin film materials, different glass substrates, thicknesses, heating times, ratios of "on times" and "off times," etc., it is required to investigate the heat distribution in the elements of the thermal printer by a numerical procedure, i.e., we require to simulate the thermal print head numerically for different values of the physical constants appearing in the mathematical model.

In our investigation, a single element of the matrix will be considered. This is not restrictive since to consider the complete matrix we merely omit the Neumann boundary conditions which we impose for the single element and apply them at the physical sides of the thermal print head.

The incident electron beam is assumed to have an electron density governed by a Gaussian distribution. Using a Cartesian coordinate system, it is described by

$$n = n_0 \exp(-2(x^2 + y^2)/a^2)$$

where a is the beam diameter at which the electron density is attenuated to $\exp(-2)$ of the density at the centre, viz., n_0. It is assumed that all the electrons have the same kinetic energy E_0 at the surface and that back scattering at interfaces is negligible. The electrons penetrate a finite distance into the print head. (This is usually arranged to be less than the thickness of the thin film, although there is no need for this.) The electrons lose energy along the penetration path. The energy E of an electron after penetrating a distance z is given by Whiddington's law (see Whiddington, Refs. [11] and [12]), viz.,

$$E^2 = E_0^2 - \beta_1 z, \qquad 0 \leqslant z \leqslant d, \tag{1}$$

and

$$E^2 = E_0^2 - \beta_1 d - \beta_2 (z - d), \qquad d \leqslant z \leqslant d + D, \tag{2}$$

where β_1 and β_2 are physical constants dependent upon the two materials and d and D are the thicknesses of the thin film and glass substrate respectively and where equations (1) and (2) are valid only for $E \geqslant 0$.

At any point z where $0 \leqslant z \leqslant d + D$ the loss of energy which has occurred will be $E_0 - E$ per electron, or

$$\epsilon = \begin{cases} n_0\{E_0 - [E_0^2 - \beta_1 z]^{1/2}\} \exp(-2(x^2 + y^2)/a^2), & 0 \leqslant z \leqslant d, \quad (3) \\ n_0\{E_0 - [E_0^2 - \beta_1 d - \beta_2 (z - d)]^{1/2}\} \exp(-2(x^2 + y^2)/a^2), & d \leqslant z \leqslant d + D, \quad (4) \end{cases}$$

for the beam.

If we assume that all the energy is dissipated in the form of heat, then the rate of heat generation will be

$$q = \frac{1}{M} \frac{d\epsilon}{dz}$$

$$= \begin{cases} \frac{1}{2M} n_0 \beta_1 [E_0^2 - \beta_1 z_1]^{1/2} \exp(-2(x^2 + y^2)/a^2), & 0 \leqslant z \leqslant d, \quad (5) \\ \frac{1}{2M} n_0 \beta_2 [E_0^2 - \beta_1 d - \beta_2 (z - d)]^{-1/2} \exp(-2(x^2 + y^2)/a^2), & d < z \leqslant d + D, \quad (6) \end{cases}$$

where we have used Eqs. (3) and (4). M is the mechanical equivalent of heat.

Thus $q(x, y, z)$ is the heat source over a period $0 \leqslant t \leqslant t_0$. When $t_0 < t$, the electron beam is switched off so that the actual heat source term for $0 \leqslant t \leqslant 2t_0$ is

$$q(x, y, z)\{1 - H(t - t_0)\},$$

where $H(\theta)$ is the Heaviside function defined by

$$H(\theta) = \begin{cases} 0, & \theta < 0, \\ 1, & \theta > 0. \end{cases}$$

A similar expression can be obtained for larger t with multiple switchings of the heat source; its form is obvious and will be omitted.

Consequently, we can now write down the partial differential equation which represents the temperature distribution $u(x, y, z, t)$ in the thermal print head where we assume for convenience that $0 \leqslant x, y, z \leqslant l$, i.e., the print head is cubic. The required equation is the combination of

$$\rho_1 c_1 \frac{\partial u}{\partial t} = K_1 \left(\frac{\partial^2 u}{\partial x^2} + \frac{\partial^2 u}{\partial y^2} + \frac{\partial^2 u}{\partial z^2} \right) + \{1 - H(t - t_0)\} \frac{n_0}{2M} \beta_1 (E_0^2 - \beta_1 z_1)^{-1/2}$$
$$\times \exp\{-2(x^2 + y^2)/a^2\} H(a^2 - (x^2 + y^2)), \qquad 0 \leqslant z \leqslant d,$$

and

$$\rho_2 c_2 \frac{\partial u}{\partial t} = K_2 \left(\frac{\partial^2 u}{\partial x^2} + \frac{\partial^2 u}{\partial y^2} + \frac{\partial u^2}{\partial z^2} \right)$$
$$+ \{1 - H(t - t_0)\} \frac{n_0 \beta_2}{2M} (E_0^2 - \beta_1 d - \beta_2 (z - d))^{-1/2}$$
$$\times \exp\{-2(x^2 + y^2)/a^2\} H(a^2 - (x^2 + y^2)), \qquad d < z \leqslant d + D,$$

where ρ_1, c_1, K_1 are the density, specific heat, and conductivity coefficients of the thin film and ρ_2, c_2, K_2 the similar coefficients for the glass substrate. By defining

$$Q(x, y, z, t) = \begin{cases} \dfrac{1}{\rho_1 c_1} \dfrac{n_0 \beta_1}{2M} (E_0^2 - \beta_1 z)^{-1/2} H(a^2 - (x^2 + y^2)) \\ \qquad \times \exp(-2(x^2 + y^2)/a^2), \qquad 0 \leqslant z \leqslant d, \\ \dfrac{1}{\rho_2 c_2} \dfrac{n_0 \beta_2}{2M} (E_0^2 - \beta_1 d - \beta_2 (z - d))^{-1/2} H(a^2 - (x^2 + y^2)) \\ \qquad \times \exp(-2(x^2 + y^2)/a^2), \qquad d < z \leqslant d + D, \end{cases}$$

and

$$K(z) = \begin{cases} K_1/\rho_1 c_1, & 0 \leqslant z \leqslant d, \\ K_2/\rho_2 c_2, & d < z \leqslant d + D, \end{cases}$$

our heat equation can be conveniently written as

$$\frac{\partial u}{\partial t} = K(z)\left(\frac{\partial^2 u}{\partial x^2} + \frac{\partial^2 u}{\partial y^2} + \frac{\partial^2 u}{\partial z^2}\right) + Q(x, y, z, t). \tag{7}$$

It can be seen from the form of K and Q that this heat equation (7) involves a discontinuous coefficient of $z(K)$, and a source term which is discontinuous in all the variables x, y, z, and t and also has a branch point either at the point

$$z = \frac{E_0^2}{\beta_1}, \qquad 0 \leqslant z \leqslant d, \tag{8}$$

or

$$z = \frac{E_0^2 - \beta_1 d}{\beta_2} + d, \qquad d < z \leqslant d + D, \tag{9}$$

only one of which, of course, can occur and beyond which (larger values of z) Q is zero.

Problems containing discontinuities in the source terms were considered in Ref. [10] where the difference schemes were found to behave well. The possible cause of difficulty in the present study is the point given by Eqs. (8) or (9). Theoretically at such a point the heat source becomes infinite.

To solve this problem of the branch point, we are faced with (at least) three alternatives.

(1) A change of variable to eliminate the branch point.

(2) Derive an analytical solution in a neighbourhood of the branch point and patch the solution obtained with the numerical solution in the rest of the region. That is, use the analytical solution on the boundary of the region around the branch point as boundary conditions for the numerical problem in the rest of the region.

(3) Neglect the branch point, in some way.

Usually we would surmise that alternative (3) was not facing the problem and that either (1) or (2) should be attempted. However, we have chosen to use approach (3) for the following reasons.

The assumption that all the energy is converted to heat is clearly an approximation to the actual physical phenomenon that takes place. Various other dissipations of energy such as electromagnetic radiation, energy lost by the emission of secondary electrons, and energy causing structural changes in the specimen may take place. (See Calbick, Ref. [1], for a discussion of the interaction of electron beams with thin films.) In the main, these dissipations will be minor

compared to the heat generation effect. However, close to the point where the energy becomes zero, the additional dissipations will have a more marked effect. That is, in a region close to the point where E becomes zero, the heat source term we have devised is not valid. In other words, in practice no branch point can occur. Since we will not know the region where the side dissipations have a significant effect we arrange for a discretization of the continuous problem so that that point where E becomes zero lies between the grid points. Hopefully, by allowing the mesh length h to be sufficiently large so that the distance from the nearest grid point to the branch point is also sufficiently large, the validity of the source term at the grid points is ensured. This construction still allows the possibility of a large source term but discounts the possibility of an infinite one. Clearly on physical grounds, this is sensible.

Consequently, we can justify not using approaches (1) and (2) above on the grounds that to eliminate by a change of variable a physically meaningless branch point is futile and to obtain an analytical solution in a small region where in that very region the uncertainty of the source is greatest, is again futile.

This solves, to a certain extent, what to do in terms of the numerical problem. We have still not eliminated the possibility of the difference scheme we propose behaving eratically in the region of $E = 0$. The numerical experiments will answer that.

We have left to impose the necessary boundary and initial conditions. These are given as follows:

$$\left.\begin{aligned} \frac{\partial u}{\partial x} &= 0, \quad x = 0, l, \quad 0 \leqslant y \leqslant l \\ \frac{\partial u}{\partial y} &= 0, \quad y = 0, l, \quad 0 \leqslant x \leqslant l \end{aligned}\right\} 0 \leqslant z \leqslant l, \tag{10}$$

$$\left.\begin{aligned} u &= \text{constant}, \quad z = l \\ \frac{\partial u}{\partial z} + h_0 u &= 0, \quad z = 0 \end{aligned}\right\} 0 \leqslant x, y \leqslant l, \tag{11}$$

and

$$u(x, y, z, 0) = g(x, y, z), \qquad 0 \leqslant x, y, z \leqslant l, \tag{12}$$

where h_0 is the convective heat transfer coefficient (see Carslaw and Jaeger, Ref. [2]) between the thin film and the air surrounding the print head, and $g(x, y, z)$ is a given function; we will take it as a given constant.

Thus our problem is to determine $u(x, y, z, t)$ satisfying Eqs. (7, 10, 11, and 12).

3. The Numerical Method

In Ref. [4] Gordon considered a novel scheme for the numerical solution of parabolic partial differential equations. In Ref. [6] Gourlay considered the method of Gordon, generalized it, and derived a theoretical basis for the method as well as proposing additional techniques based upon the generalized method (see also Gourlay and McGuire [7] and McGuire [9]). Gourlay's method has been named the Hopscotch scheme because of the way in which the computation proceeds. We will consider a three-space-dimensional version of this method for the numerical solution of our physical problem. To do this we need some notation.

A rectalinear grid is superimposed on the region of computation, viz., $(0 \leqslant x, y, z \leqslant l) \times (0 \leqslant t \leqslant T)$, where we assume the mesh spacings in the space coordinates are equal, viz.,

$$\Delta_x = \Delta_y = \Delta_z = h,$$

and the mesh spacing in the time coordinate is τ. The mesh ratio is assumed constant and equal to r. We denote by u_{ijk}^m the value of the unknown function u at the point $(ih, jh, kh, m\tau) = (x, y, z, t)$ for $i, j, k = 0, 1, \ldots, N$, $Nh = l$, $m = 0, 1, 2, \ldots$ and similarly Q_{ijk}^m for Q. We define the difference operators δ_x, δ_y, δ_z as the usual central difference operators, where

$$\delta_x u_{ijk}^m = u_{(i+1/2)jk}^m - u_{(i-1/2)jk}^m$$

with similar expressions for δ_y and δ_z. We further denote by L the differential operator $K(z)(\partial^2 u/\partial x^2 + \partial^2 u/\partial y^2 + \partial^2 u/\partial z^2)$ and by L_h the difference approximation to L. Thus Eq. (7) can be written as

$$\frac{\partial u}{\partial t} = Lu + Q(x, y, z, t).$$

The finite difference method which is the obvious three-dimensional counterpart of the scheme of Ref. [6] can be written as

$$\begin{aligned} u_{ijk}^{m+1} &= u_{ijk}^m + \tau(L_h u_{ijk}^m + Q_{ijk}^m) \qquad \text{for } i + j + k + m \text{ even}, \\ u_{ijk}^{m+1} &= u_{ijk}^m + \tau(L_h u_{ijk}^{m+1} + Q_{ijk}^{m+1}) \qquad \text{for } i + j + k + m \text{ odd}. \end{aligned} \tag{13}$$

Eq. (13) can be written in the more convenient form

$$u_{ijk}^{m+1} - \tau\theta_{ijk}^{m+1}[L_h u_{ijk}^{m+1} + Q_{ijk}^{m+1}] = u_{ijk}^m + \tau\theta_{ijk}^m[L_h u_{ijk}^m + Q_{ijk}^m], \tag{14}$$

where

$$\theta_{ijk}^{m} = \begin{cases} 1 & \text{if } m+i+j+k \text{ is odd,} \\ 0 & \text{if } m+i+j+k \text{ is even.} \end{cases}$$

The computational algorithm proceeds exactly as described in Ref. [6]. Namely, for those points corresponding to $\theta_{ijk}^{m+1} = 0$, Eq. (14) is applied to calculate alternate nodal points u_{ijk}^{m+1} by an explicit scheme. Having found these values, the remaining u_{ijk}^{m+1} corresponding to those points for which $\theta_{ijk}^{m+1} = 1$ are calculated by what looks like an implicit scheme but, in fact, will be explicit in nature if the difference operator is of a class of E operators as defined by Gourlay in Ref. [6]. Such an E operator is the usual simple difference approximation

$$L_h = \frac{K(kh)}{h^2}(\delta_x^2 + \delta_y^2 + \delta_z^2).$$

Substituting this expression for L_h into Eq. (14) will show that for $\theta_{ijk}^{m+1} = 1$, those points about u_{ijk}^{m+1} which usually make the scheme implicit have already been calculated by Eq. (14) with $\theta_{ijk}^{m+1} = 0$, so that the scheme is computationally explicit.

Gourlay [6] in a clever bit of manipulation, noticed that when Eq. (13) was considered in the form (14), by an additional application of (14) with m replaced by $m + 1$, the resulting schemes could be combined to give

$$u_{ijk}^{m+2} - \tau\theta_{ijk}^{m+2}[L_h u_{ijk}^{m+2} + Q_{ijk}^{m+2}] = 2u_{ijk}^{m+1} - (u_{ijk}^{m} + \tau\theta_{ijk}^{m}[L_h u_{ijk}^{m} + Q_{ijk}^{m}]). \quad (15)$$

Now Eq. (15) reduces to the simple explicit scheme

$$u_{ijk}^{m+2} = 2u_{ijk}^{m+1} + u_{ijk}^{m}$$

when $\theta_{ijk}^{m+2} = \theta_{ijk}^{m}$ is zero. Consequently, for half the points, an extremely simple substitution attains the approximation required at the next level of time. Having calculated these nodal values, Eq. (15) is then applied with $\theta_{ijk}^{m+2} = \theta_{ijk}^{m} = 1$ to obtain the remaining values of u_{ijk}^{m+2}.

We have described this part of the computational method (the full details may be found in Ref. [6]) to stress the point that the Hopscotch algorithm (14) not only allows one to dispense with the usual tridiagonal conversions but also allows the writing of an exceedingly fast algorithm whereby only half of the nodal values have any substantial computation attached to them. For the E operator described above, the method is unconditionally stable and has a local accuracy of $O(h^2 + \tau)$. By virtue of the method, no intermediate boundary conditions are required, so no boundary correction techniques like those described in Ref. [8] are needed.

Thus, Eq. (15) is applied to points with $i, j, k = 0, 1, \ldots, N$, where for $i = 0, N$, $j = 0, N$, the normal boundary conditions are applied by using the simple difference replacements

$$\frac{\partial u}{\partial x}\Big|_{x=0} = \frac{u^m_{+1jk} - u^m_{-1jk}}{2h}, \qquad \frac{\partial u}{\partial x}\Big|_{x=l} = \frac{u^m_{(N+1)jk} - u^m_{(N-1)jk}}{2h},$$

etc. For $k = N$ the simple Dirichlet condition $u = 0$ is incorporated. At $k = 0$ the third boundary condition $\partial u/\partial z = -h_0 u$ is used, where $\partial u/\partial z\,|_{z=0}$ is replaced in a similar fashion to the derivatives above.

4. Numerical Results

A series of numerical experiments was conducted to test the behaviour of the difference method (15) upon the physical problem (7). In order to test the programmes and to discover the behaviour of the finite difference schemes in the neighbourhood of a singularity, we devised a problem for which a theoretical solution could be determined. Consider the partial differential equation

$$\frac{\partial u}{\partial t} = K\left(\frac{\partial^2 u}{\partial x^2} + \frac{\partial^2 u}{\partial y^2} + \frac{\partial^2 u}{\partial z^2}\right) + 2\zeta \cos \pi x \cos \pi y(\psi - z)^{-2m}$$
$$\times [\pi^2(1 - z) - m(2m + 1)(\psi - z)^{-2}(1 - z) + 2m(\psi - z)^{-1}] \quad (16)$$

subject to the boundary conditions

$$\left\{\frac{\partial u}{\partial x} = 0, \quad x = 0, 1; \quad 0 \leqslant y \leqslant 1; \quad \frac{\partial u}{\partial y} = 0, \quad y = 0, 1; \quad 0 \leqslant x \leqslant 1\right\} \quad 0 \leqslant z \leqslant 1,$$

$$u = 0, \quad z = 1, \quad 0 \leqslant x, y \leqslant 1; \quad \frac{\partial u}{\partial z} = -h_0 u, \quad z = 0; \quad 0 \leqslant x, y \leqslant 1,$$

and the initial condition

$$u(x, y, z, 0) = \cos \pi x \cos \pi y[\sin \pi\alpha(z + \beta) + \zeta(\psi - z)^{-2m}(1 - z)],$$

where K and ζ are constants, ψ is a parameter chosen to place the singularity so that it occurs between mesh points, and m is a parameter chosen to give the source function and solution required properties; in our case we chose $m = \frac{1}{2}$, α and β are parameters which satisfy

$$\alpha = 2 - \frac{1}{\pi}\tan^{-1}(\phi), \quad (17)$$

$$\beta = \frac{1}{\alpha\pi}\tan^{-1}(\phi), \quad (18)$$

where

$$\phi = \tan \pi\alpha\beta, \tag{19}$$

$$h_0 = \pi\alpha/\phi, \tag{20}$$

and

$$2m/\psi - 1 = h_0 . \tag{21}$$

Clearly the expression (19) for ϕ is nonlinear. Using Eqs. (17, 20, 21), we can obtain that

$$\phi = \frac{\pi}{\left(\frac{2m}{\psi} - 1\right)} \left[2 - \frac{1}{\pi} \tan^{-1}(\phi)\right].$$

To solve this equation for ϕ we use the Newton–Raphson method, viz.,

$$\phi_{i+1} = \phi_i - \frac{\left[\phi_i + \frac{\pi}{\left(1 - \frac{2m}{\psi}\right)} \left(2 - \frac{1}{\pi} \tan^{-1}(\phi_i)\right)\right]}{\left[1 - \frac{1}{\left(1 - \frac{2m}{\psi}\right)(1 + \phi_i^2)}\right]}. \tag{22}$$

To solve Eq. (22) we need an initial estimate to ϕ, ϕ_0. We used $\psi = 0.45$ for our numerical example and so with $m = 0.5$ we took the initial value of ϕ to be $\phi_0 = 4.0$; this ensures that the associate constant h_0 is positive. After iteration so that successive iterates agreed to within 10^{-4} it was found that the required value of ϕ was 4.0535. Substituting this value of ϕ into Eqs. (17 and 18), α and β could then be determined. Consequently, h_0 could be calculated and as a final check on the accuracy of ϕ, ψ was recalculated from the values of α and β. It was found to agree exactly (to eight decimal places).

With these definitions, the solution to Eq. (16) is

$$u = \cos \pi x \cos \pi y[e^{-\gamma t} \sin \pi\alpha(z + \beta) + \zeta(\psi - z)^{-2m}(1 - z)], \tag{23}$$

where $\gamma = \pi^2 K(2 + \alpha^2)$. That Eq. (23) is a solution to Eq. (16) and the associated boundary and initial conditions can easily be checked by differentiating u from (23) and using the definitions (17–21).

The difference scheme (15) was used to calculate the solution of (16) for several values of the mesh ratio r where the source term is "on" for all time, and valid for $0 \leqslant x, y, z \leqslant 1$. The solution was computed to 50 time steps when the maximum

TABLE I

Maximum Errors at 50 Time Steps for $m = 0.5$, $\psi = 0.45$, and $z = 0$, (0.1), 0.9, where Theoretical Solution Was Used at $z = 1.0$

Errors
6.1382×10^{-4}
2.58086×10^{-3}
1.90295×10^{-3}
1.65232×10^{-3}
9.62693×10^{-3}
6.46465×10^{-3}
8.2443×10^{-4}
3.25166×10^{-3}
3.32104×10^{-3}
1.88148×10^{-3}

error for several values of z is shown in Table I. $r = 3.0$ and the theoretical solution is of order one. As can be seen from the table, the errors are small and, even in the neighbourhood ($z = 0.4$ and 0.5) of the singular point, the errors are still of the order of 10^{-3}.

Having satisfied ourselves that the program was indeed working and behaved well in the region of the singular point, we performed several experiments upon the physical problem described in Section 2. We chose the physical constants to yield a large range of temperatures; from 0 to about 1500°C. In this manner it was hoped that any difficulties which arose out of large fluctuations of tempera-

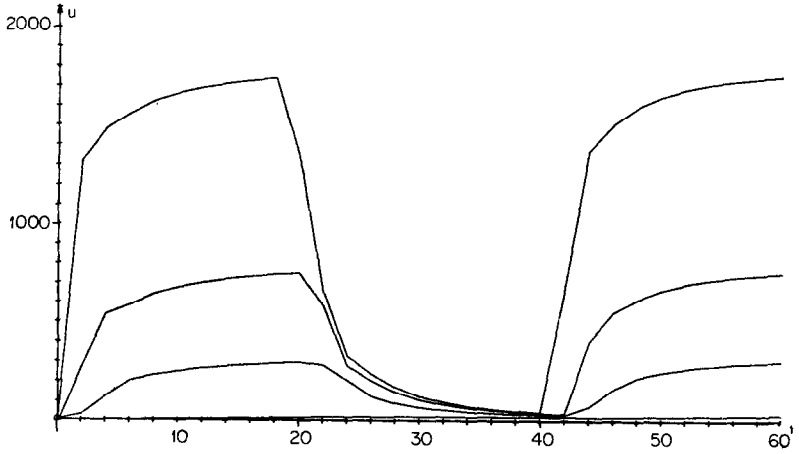

FIG. 3. Graphs of temperature distribution in thermal print head for a printing cycle of 40τ with on–off ratio = 2.

ture would show up in the numerical results. The results of these experiments are shown in Figs. 3–11, where a complete range of situations has been covered.

In the results that follow, the radius of the electron beam was taken as 0.2. The results quoted in the graphs are for $x = y = 0.5$. Figure 3 shows the results from time $t = 0$ up to $t = 60\tau$ where τ was taken equal to 0.005 so that the mesh ratio r was 0.5. The electron beam was switched off after 20τ and switched on again after 40τ. We define the ratios of the printing cycle to the time for which the heat is on as the "on–off" ratio. Thus in this case the on–off ratio was two.

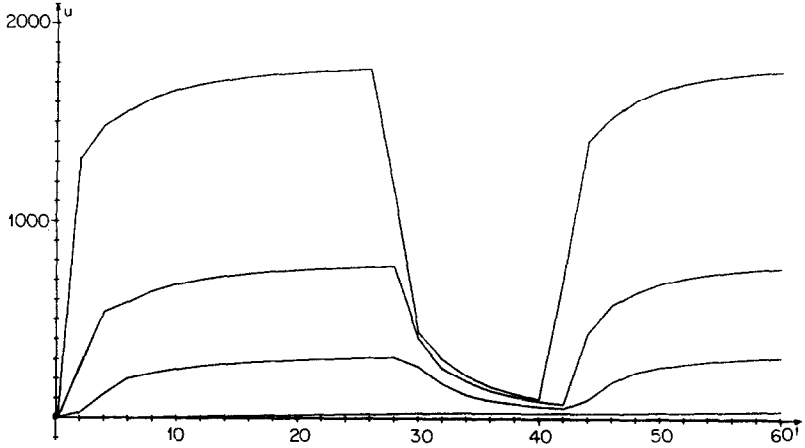

FIG. 4. Graphs of temperature distribution in thermal print head for a printing cycle of 40τ with on–off ratio = 1.5.

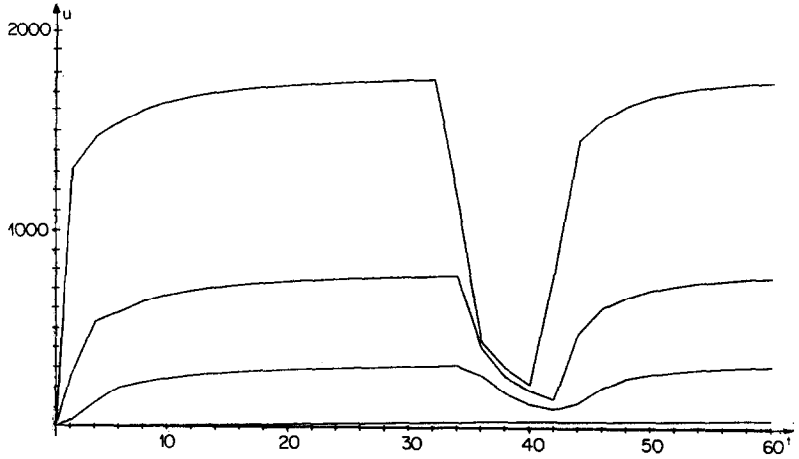

FIG. 5. Graphs of temperature distribution in thermal print head for a printing cycle of 40τ with on–off ratio = 1.25.

The graphs show the temperatures in the layers $z = 0, 0.1, 0.2, 0.3$ in decreasing magnitude, where for lower layers the temperature is very small so that on the scale used no graphs appear. The branch point was taken as $z = 0.05$ so that the source term had only a positive value for $z = 0.0$. The thickness d of the thin film was taken as 0.2 opposed to the total thickness of the element being 1.0. The curves are those actually produced by the computer graph plotter where straight lines were used to connect successive computed points. The computed solution is clearly well-behaved.

Figure 4 shows results similar to the experiment of Fig. 3 except the "on–off" ratio was taken to be 1.5 so that the heat source was not switched off until 30τ. The heat source was again switched on at 40τ. The computed solution is again well-behaved.

Figure 5 reduces still further the on–off ratio to 1.25. The printing cycle was again 40τ.

Comparing Figs. 3, 4, and 5 shows that the only significant difference in prolonging the heating process is to raise very slightly the upper temperature achieved. In all cases, when the heat is switched off the temperature drops very rapidly. The problems were run for a longer period of time than that suggested by the graphs and in no case was there a build up of temperature in the print head.

Figure 6 shows an example of more than a single switching of the heat source. The printing period has been reduced to 20τ. The computed results again extend to 60τ and the on–off ratio is two.

Figure 7 has a similar printing cycle to Fig. 6 except the on–off ratio is four, i.e., the beam is on for less time than it is off.

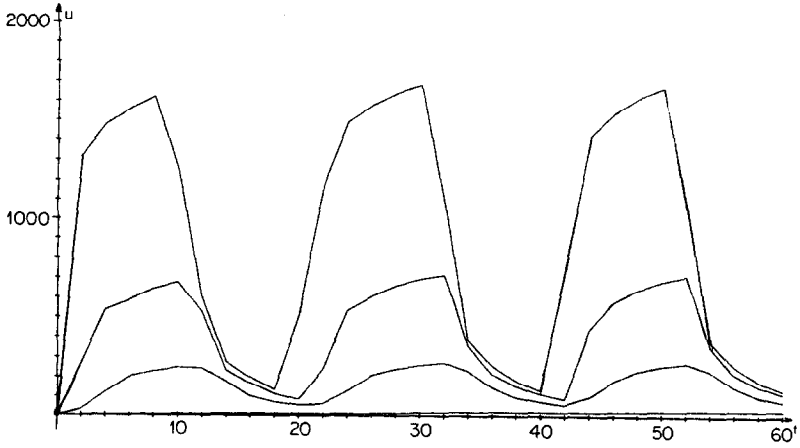

FIG. 6. Graphs of temperature distribution in thermal print head over several printing cycles each of 20τ duration with on–off ratio = 2.

Figure 8 shows a further reduction in the printing period. The computed results still extend to 60τ with an on–off ratio of two. The printing cycle was 10τ.

Figure 9, with a reduced vertical scale to conserve space, shows the effect of applying an on–off ratio of four to the printing cycle of 10τ.

Figures 10 and 11 show the graphs obtained from a very rapid switching of the heat source. The printing cycle is 4τ. For the graphs in Fig. 10, the on–off ratio is two, for those in Fig. 11 the on–off ratio is four.

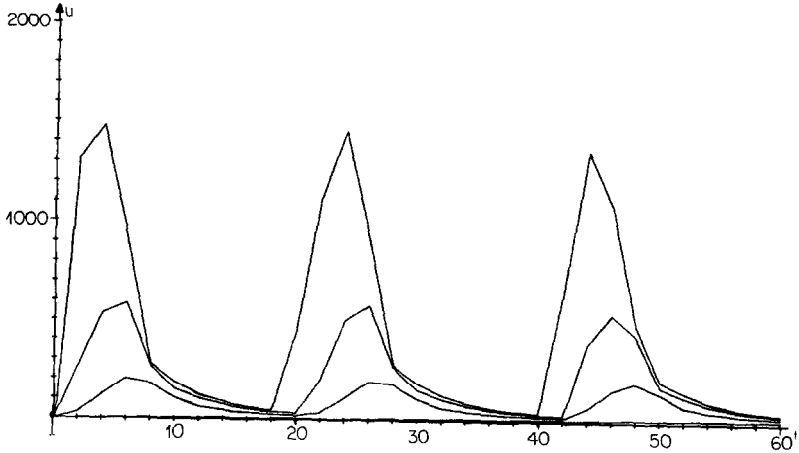

FIG. 7. Graphs of temperature distribution in thermal print head with printing cycle = 20τ and on–off ratio = 4.

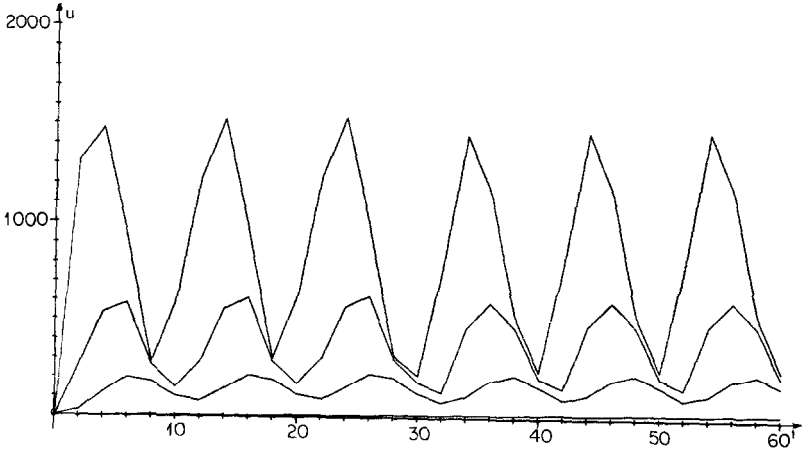

FIG. 8. Graphs of temperature distribution in thermal print head with printing cycle = 10τ and on–off ratio = 2.

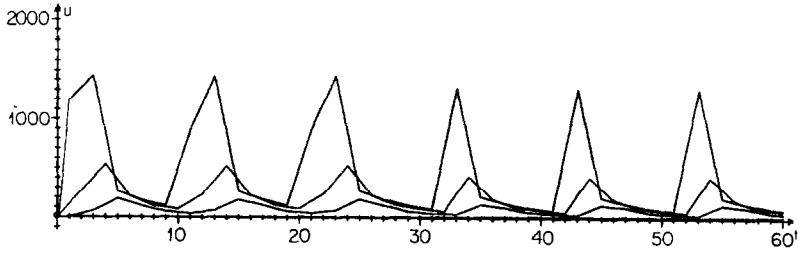

FIG. 9. Graphs with a reduced vertical scale of temperature distribution in thermal print head with printing cycle = 10τ and on–off ratio = 4.

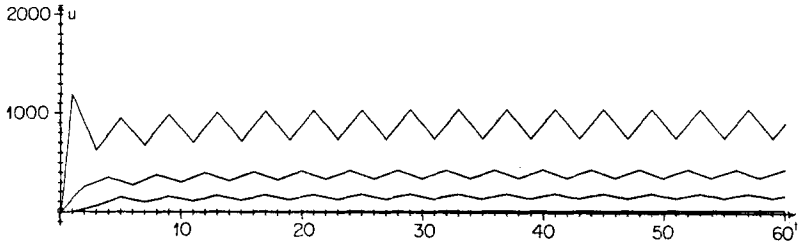

FIG. 10. Graphs of temperature distribution in thermal print head with printing cycle = 4τ and on–off ratio = 2.

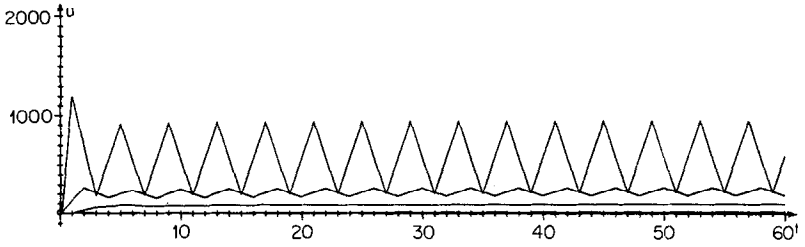

FIG. 11. Graphs of temperature distribution in thermal print head with printing cycle = 4τ and on–off ratio = 4.

In all cases, exceedingly good results have been obtained and are representative of what one would expect in practice. (However, see Section 5.) The experiments reported above represent just a few of the numerical experiments carried out. From these and other numerical experiments like them, a manufacturer could achieve a required pattern of temperature distributions in a projected thermal print head merely by changing the printing periods, the on–off ratios, or other physical constants defining the thin film and glass substrate.

5. Concluding Remarks

As mentioned in the previous section, many more numerical experiments were carried out than those reported here. In all cases, the model was three-space-dimensional with 1000 points taken to represent the unit cube. The algorithm took on the average 50 sec to compute 10 time steps when the print out was required every 10 time steps and went up to 50 sec for 6 time steps when print out was required at each time step; this increase being by virtue of the computational method [6] rather than increased printing time. In contrast, the A.D.I. scheme reported in Ref. [10] would take approximately ten times as long to compute the same points. Consequently, using the A.D.I. schemes would mean a severe curtailment in the number of experiments which could be performed. Further, the developmental work required to use the Hopscotch scheme is considerably less than the A.D.I. schemes. Clearly, for the excellent results obtained, the developmental and computational aspects of the Hopscotch scheme make it a very attractive scheme to use for the complicated physical problems in several space dimensions as exemplified by the physical problem in Section 2.

We must, however, end this paper on a note of warning. It has been found for certain combinations of the physical constants used taken in conjunction with the size of the mesh ratio being large, that *meaningless* results can be obtained. This effect can be obtained even with a homogeneous partial differential equation when the exponential function in the solution has a large negative argument. These effects, of course, are due to the local truncation error (for those physical constants and mesh ratios alluded to above) being large. That is, although the difference scheme is unconditionally stable, in certain circumstances the local truncation error becomes so large so as to swamp the true solution. In this case, by the incorporation of a suitable error control similar to those currently used in the solution of ordinary differential equations, the local truncation error can be kept small, i.e., by a reduction of the mesh ratio in the neighbourhood of large local truncation errors.

We mention this aspect out of interest only since, for the physical problem, we have considered it was necessary to take a small mesh ratio and particular physical constants which did *not* give rise to the above-mentioned behaviour. This behaviour has received considerable attention in the numerical solution of ordinary differential equations but, to our knowledge, very little attention in partial differential equations.

Acknowledgments

The author wishes to express his gratitude to the National Cash Register (Manufacturing) Co. Ltd. of Dundee for the financial support during the period when this work was carried out.

The discussions with Dr. A. R. Gourlay, I.B.M. Research Laboratories, Peterlee, England, on the Hopscotch schemes are also gratefully acknowledged.

REFERENCES

1. C. J. CALBRICK, Interaction of electron beams with thin films, *in* "Physics of Thin Films" (G. Hass and R. E. Thun, Eds.), Vol. 2, Academic Press, New York, 1964.
2. H. S. CARSLAW AND J. C. JAEGER, "Conduction of Heat in Solids," Oxford Univ. Press, London, 1947.
3. A. FRIEDMAN, "Partial Differential Equations of Parabolic Type," Prentice Hall, Englewood Cliffs, N. J., 1964.
4. P. GORDON, *J. Soc. Ind. Appl. Math.* **13** (1965).
5. A. R. GOURLAY, The numerical solution of evolutionary partial differential equations, *in* "Proceedings of the Conference on the Numerical Solution of Differential Equations" (J. Ll. Morris, Ed.), Vol. 109, Lecture notes in Mathematics, Springer-Verlag, New York/ Berlin, 1969.
6. A. R. GOURLAY, A fast, second-order partial differential equation solver, to appear.
7. A. R. GOURLAY AND G. R. MCGUIRE, General hopscotch algorithms for the numerical solution of partial differential equations, to appear.
8. A. R. GOURLAY AND A. R. MITCHELL, Intermediate boundary correction for split operator methods in three dimensions, *BIT* **7** (1967).
9. G. R. MCGUIRE, Masters thesis, University of Dundee, 1969.
10. J. Ll. MORRIS, On the numerical solution of a heat equation associated with a thermal print head. I, *J. Comp. Phys.* **5** (1970), 208.
11. R. WHIDDINGTON, *Proc. Roy. Soc. Ser. A* **86** (1912).
12. R. WHIDDINGTON, *Proc. Cambridge Phil. Soc.* **16** (1912).